ERLANGEN CENTRE FOR ASTROPARTICLE PHYSICS

FRIEDRICH-ALEXANDER UNIVERSITÄT ERLANGEN-NÜRNBERG
FACULTY OF SCIENCES

# *Low luminosity X-ray sources in the old populations of dwarf galaxies and globular clusters*

*Sara Saeedi*


***FRANCI Meeting***

***October 14th, 2021***

- Old stellar populations:
  Glabular clusters
  Nearby dwarf spheriodal galaxies
- The nature of low luminosity X-ray sources in the globular clusters and dwarf spheroidal galaxies.
- X-ray luminosity functions of the old populations.
- Recent *eROSITA* study of 47 Tuc globular cluster.
- Recent *XMM-Newton* and *eROSITA* studies of the spheroidal dwarf galaxies.

# Globular clusters in the Milky Way

**Globular clusters (GCs):**

- Spherical shaped, compact, old, and bright accumulations of stars, mainly observed in the halo, thick disk, and the bulge of the Galaxy.
- The dynamical structure of the GCs is ideal for the formation of a large number of binary systems.
- There are 150 GCs in Milky Way. Located at distances from ~2 to ~30 kpc from us.
- 8 persistently luminous low mass X-ray binaries (LMXBs) has been classified in the GCs.
- Studies shows noticeable number of low luminosity X-ray sources, what are these sources?

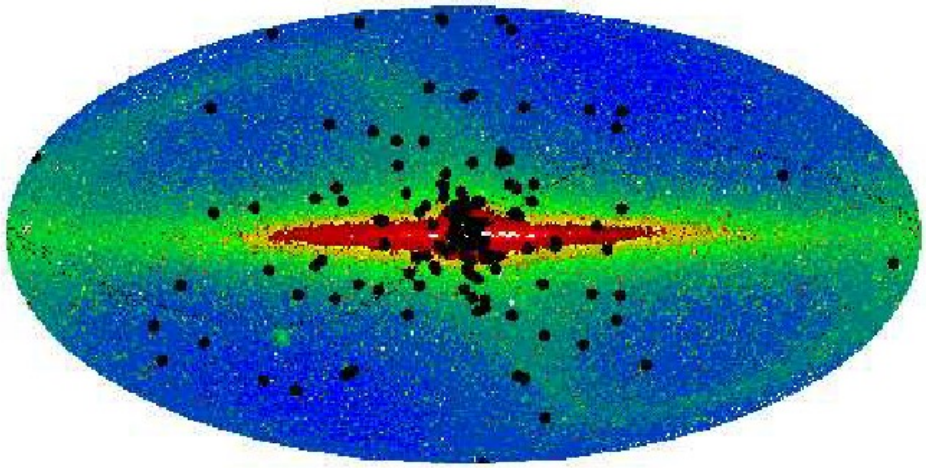

Globular cluster distribution about the galaxy. Positions are from Harris (et al. 1996). plotted as black circles on top of the COBE FIRAS 2.2 micron map of the Galaxy using a Mollweide projection. (Credit COBE survey).

# Low luminosity X-ray sources in globular clusters

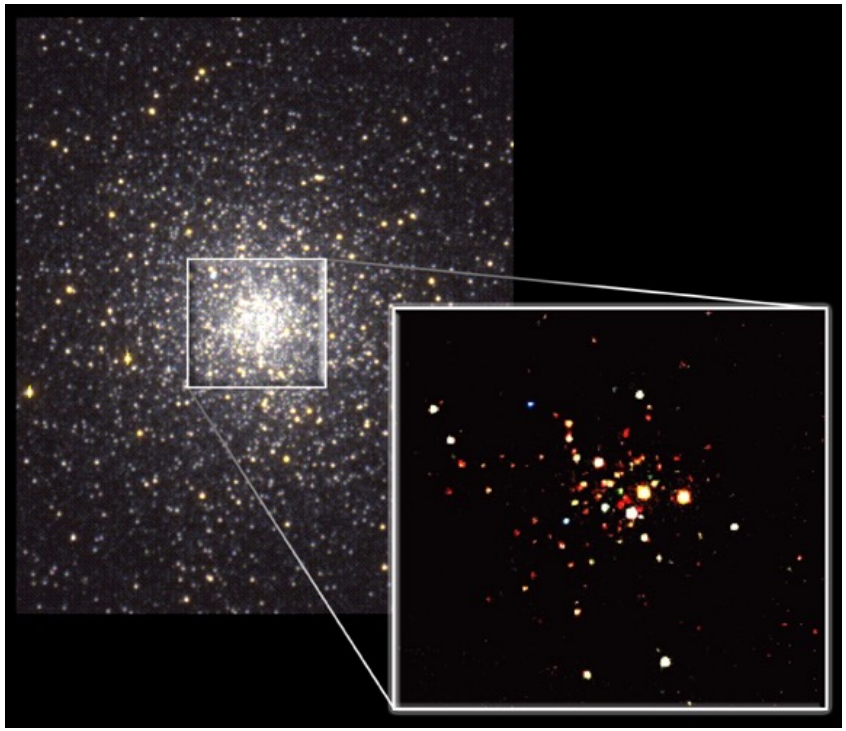

The composite image shows the scale of the Chandra image of 47 Tucanae in comparison to ground-based, optical observations.

(Credit: Optical: ESO/Danish 1.54-m/W. Keel et al., X-ray: NASA/CfA/J. Grindlay et al.)

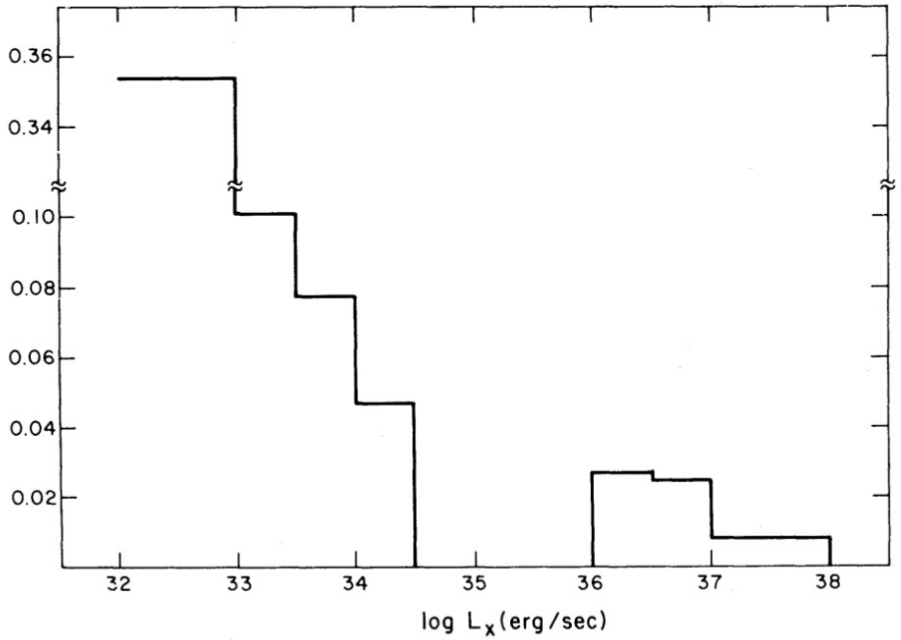


The normlized maximum likelihood X-ray luminosity function for glabular clusters in the energy range of 0.5-4.5 keV based on the data of 71 glabular clusters observed by *Einstein* observatory. (Hertz and Grindlay, 1983, APJ)

# What are low luminosity X-ray sources?

**The main population of X-ray sources: Lx <$10^{35}$ erg/s**

- **Quiescent low mass X-ray binaries (QLMXBs)**
- **Different types of accreting white dwarfs (AWDs)**
  - **Symbiotic Stars**
  - **Cataclysmic Variables (CVs)**
- **Radio millisecond pulsars (MSP)**
- **Magnetically active binary systems**

| Source class | Spectral emission keV | Luminosity erg $s^{-1}$ |
|---|---|---|
| Symbiotic: $\alpha$-type | <0.5 | $L_{bol} > 10^{36}$ |
| Symbiotic: $\beta$-type | <2.4 | $L_x \sim 10^{30-32}$ |
| Symbiotic: $\delta$-type | >2.4 | $L_x \sim 10^{31-34}$ |
| Symbiotic: $\gamma$-type | >2.4 | $L_x > 10^{34}$ |
| CV: Non-magnetic | 2.–5. | $L_x \sim 10^{29-32}$ |
| CV: Polars | <5.0 | $L_{bol} \sim 10^{30-31}$ |
| CV: Intermediate polars | 5.–50. | $L_x < 10^{34}$ |
| Quiescent LMXBs | <5. | $L_x \sim 10^{31-33}$ |
| Millisecond pulsars | 0.2–2.5 | $L_x \sim 10^{30-31}$ |
| Active binaries | <2.5 | $L_x \sim 10^{29-32}$ |

# Methods of the classification of X-ray sources

**Methods of classification:**

- **X-ray analysis:**
  - Timing analysis (variability, periodicity, pulsation)
  - Spectral analysis
  - X-ray hardness ratio study
- **Multi-wavelength study of the source counterpart(s)**
  - Counterparts in optical/ infrared/ UV
  - Colour-colour and colour/magnitude diagrams
  - X-ray to optical flux ratio

# *eROSITA* Observations of 47 Tuc

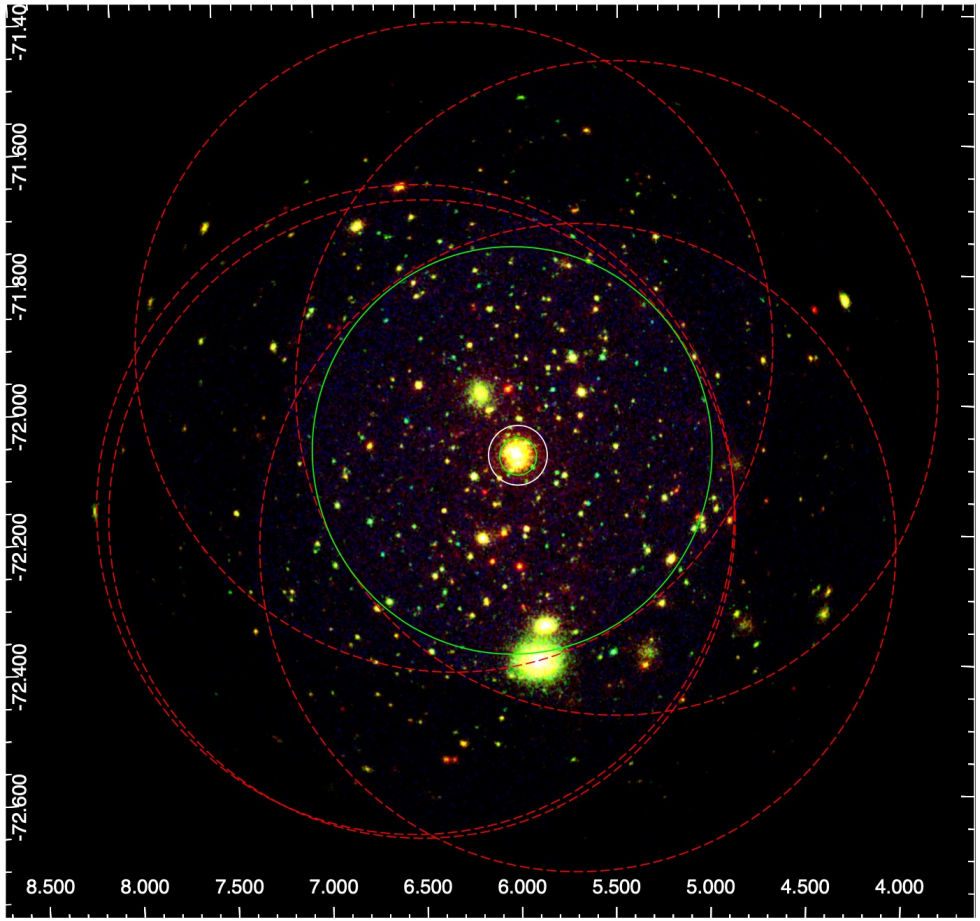


Combined X-ray image of *eROSITA* observations in the field of 47 Tuc with a total radius of 42′.
**White region:** half-mass radius of 47 Tuc.
**Red regions:** regions observed by five *eROSITA* observations.
**Green regions:** with radii of 18′.8 and 1′.7, show the area, which is covered by all observations and the extent of the unresolved emission from the centre of 47 Tuc.

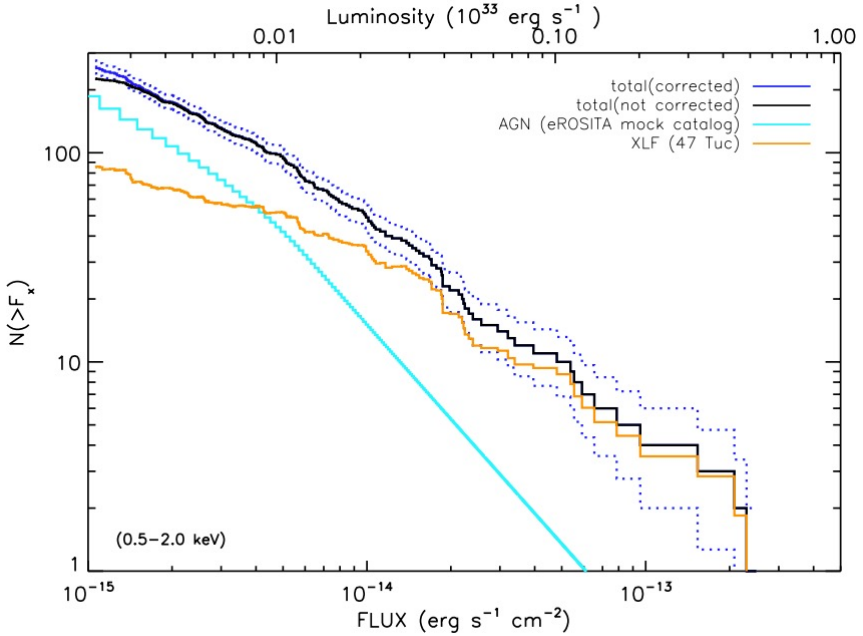


X-ray luminosity function of 47 Tuc according to *eROSITA* observations.
These sources can mainly be candidates for quiescent low LMXBs and different types of accreting white dwarfs, especially symbiotic stars.

Saeedi et al, 2021, submitted in A&A

# Multi-wavelength studies of counterparts

Multi-wavelength counterparts of the sources has been checked in several surveys/catalogues. Two samples of infrared(WISE survey) and optical (Gaia survey) counteroarts are shown here:

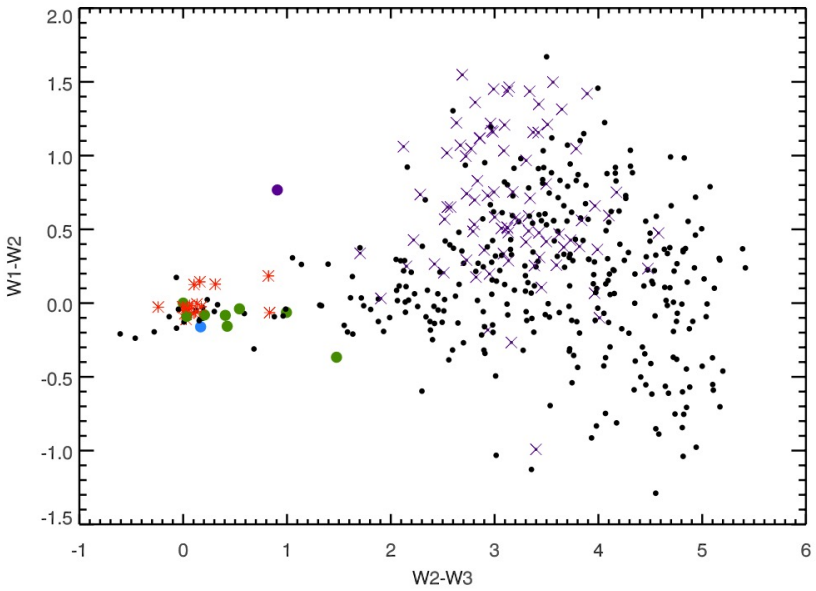


Colour-colour diagram of mid-infrared WISE. (Colours according to Wright et al. 2010)
×: AGNs
✳: Foreground satrs
●: Source with counterpart classified as RGBs in 47Tuc
●: Main sequence member of 47 Tuc
●: Unclassfied sources

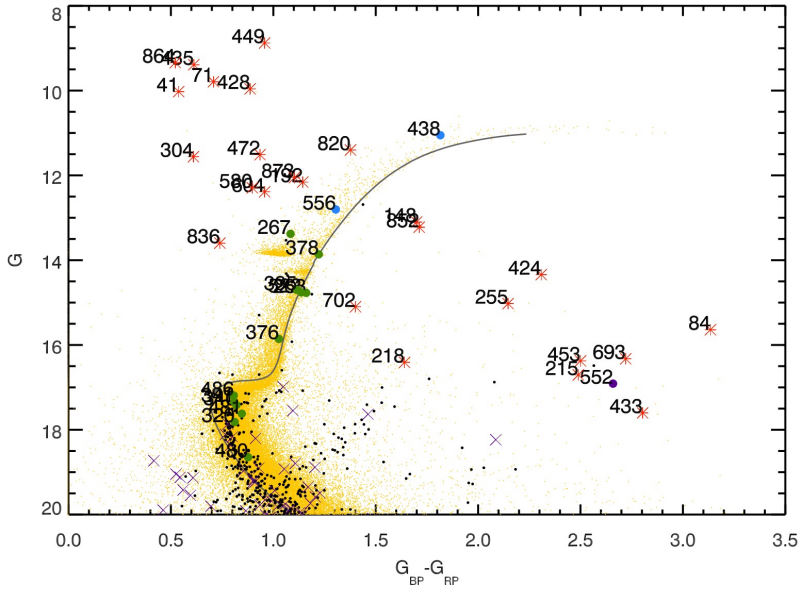


The optical counterpart of the X-ray sources in the field of 47 Tuc dSph observed by Gaia third data released (Gaia Collaboration 2020).

Saeedi et al, 2021, submitted in A&A

# X-ray Analysis of *eROSITA* data of 47 Tuc

- In 4 energy bands: 0.2–0.6 keV, 0.6–1.1 keV, 1.1–2.3 keV, and 2.3–5.0 keV.
- Hardness ratio measurement was significant, only if the detection likelihood for the both corresponding energy bands was higher than 6 (i.e, >3σ).
- Lines represent the hardness ratios of different spectral models with various column densities from NH=$10^{20}\ cm^{-2}$ to NH= $10^{23}\ cm^{-2}$.

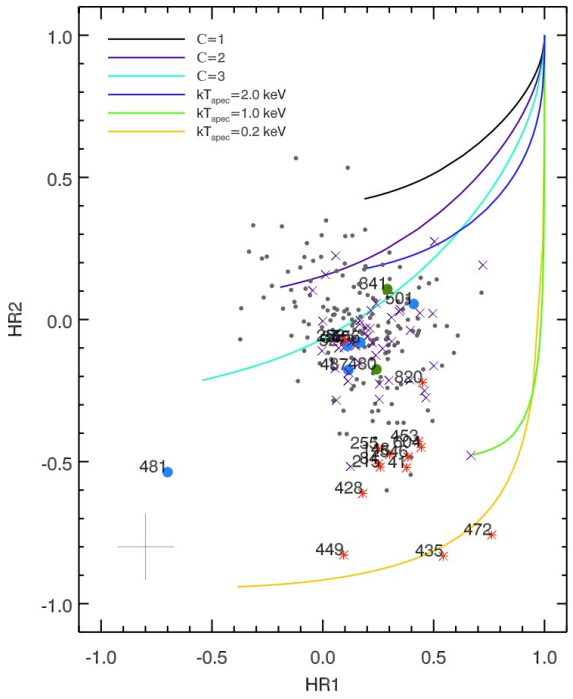


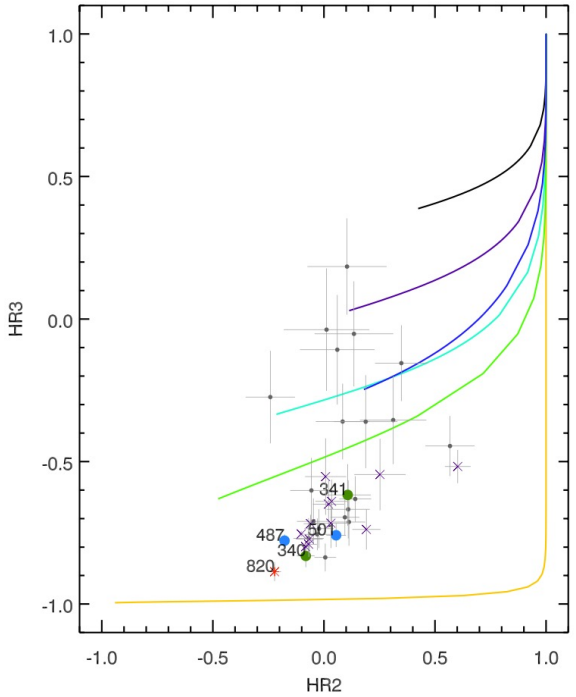


×: AGNs

✳: Foreground satrs

●: Source with counterpart classified as RGBs in 47 Tuc

●: Main sequence member of 47 Tuc

●: Unclassfied sources

Saeedi et al, 2021, submitted in A&A

# X-ray Analysis of *eROSITA* data of 47 Tuc

## Spectral analysis:

- X-ray spectral analysis for the bright sources with optical/infrared counterparts classified as a member of 47 Tuc, plus the most variable foreground star.
- Merging the spectra of all observations helped to improve the statistics.

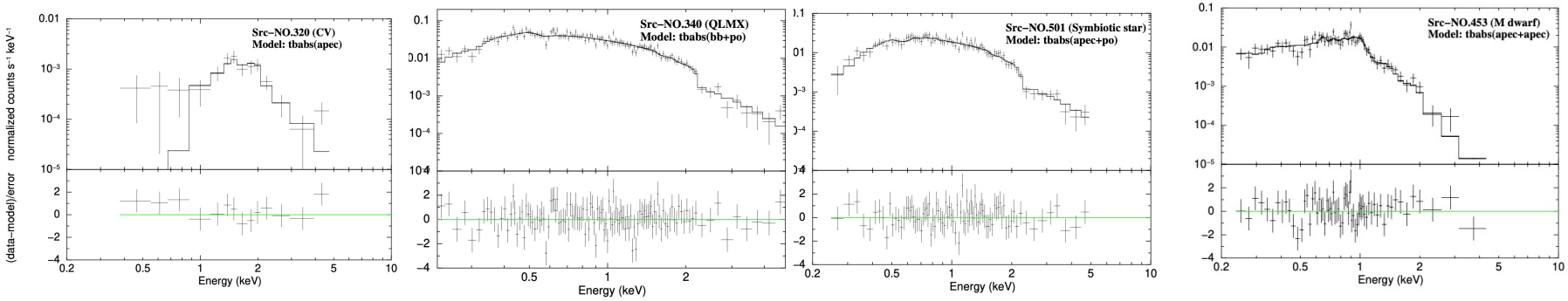


| Src-No | Model | $N_H$ $10^{22}$ cm$^{-2}$ | Photon index | *Temperature* | Abundance | $\chi^2$ (d.o.f) | Unabsorbed $F_X$ $10^{-14}$erg s$^{-1}$ cm$^{-2}$ | Unabsorbed $L_X^*$ erg s$^{-1}$ |
|---|---|---|---|---|---|---|---|---|
| 320 | tbabs×(apec) | $1.85^{+0.59}_{-1.25}$ | – | >1.32 keV | – | 1.15 (10) | $5.20^{+0.88}_{-0.87}$ | $1.23 \times 10^{32}$ |
| 340 | **tbabs×(bb+po)** | $0.04^{+0.015}_{-0.01}$ | $\mathbf{2.23^{+0.33}_{-0.30}}$ | **< 0.90 keV** | | **1.05 (116)** | $12.38^{+1.10}_{-0.98}$ | $2.80 \times 10^{32}$ |
| | **tbabs×(nsa+po)** | **<0.05** | $\mathbf{2.06^{+0.08}_{-0.14}}$ | **log(T): $5.8^{+0.13}_{-0.29}$ K** | | **0.97 (116)** | $9.27^{+0.27}_{-0.26}$ | $2.14 \times 10^{32}$ |
| 501 | **tbabs×(apec+apec)** | $0.05^{+0.03}_{-0.02}$ | – | $T1 : 0.30^{-0.08}_{+0.60}$ keV | – | 1.27 (80) | $6.14^{+0.26}_{-0.25}$ | $1.49 \times 10^{32}$ |
| | | | | $T2 : 5.41^{+13.2}_{-2.08}$ keV | | | | |
| 453 | tbabs×(apec+apec) | $0.020^{+0.02}_{-0.03}$ | – | $T1 : 0.28^{+0.09}_{-0.05}$ | $0.17^{+0.09}_{-0.06}$ | 1.07 (58) | $2.34^{+0.12}_{-0.11}$ | $1.12\times10^{29**}$ |
| | | | | $T2 : 1.04^{+0.09}_{-0.10}$ | | | | |

∗: We assumed a distance of 4.45 kpc to estimate the X-ray luminosity of sources in 47 Tuc
∗∗: For Src-No. 453, the distance of the counterpart, which is a foreground star located at ~200 pc is considered.

# *eROSITA* Observations of 47 Tuc

FRIEDRICH-ALEXANDER UNIVERSITÄT ERLANGEN-NÜRNBERG
FACULTY OF SCIENCES

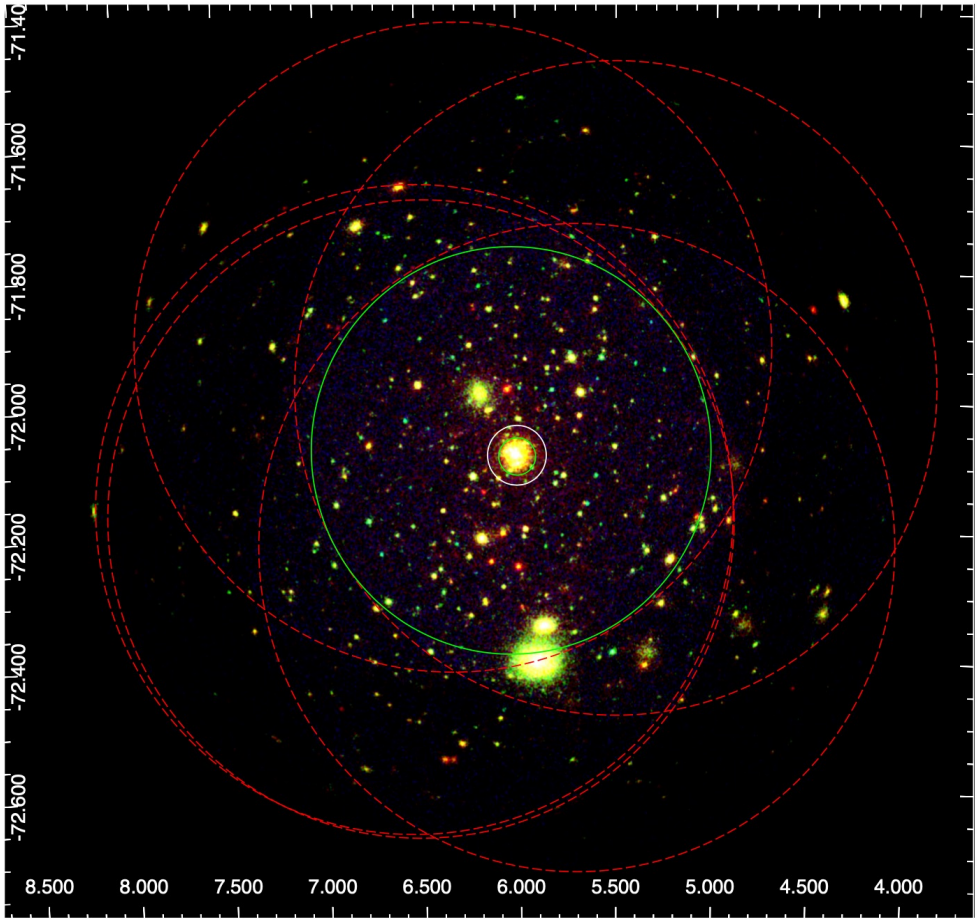


Combined X-ray image of *eROSITA* observations in the field of 47 Tuc with a total radius of 42′.
**White region:** half-mass radius of 47 Tuc.
**Red regions:** regions observed by five *eROSITA* observations.
**Green regions:** with radii of 18′.8 and 1′.7, show the area, which is covered by all observations and the extent of the unresolved emission from the centre of 47 Tuc.

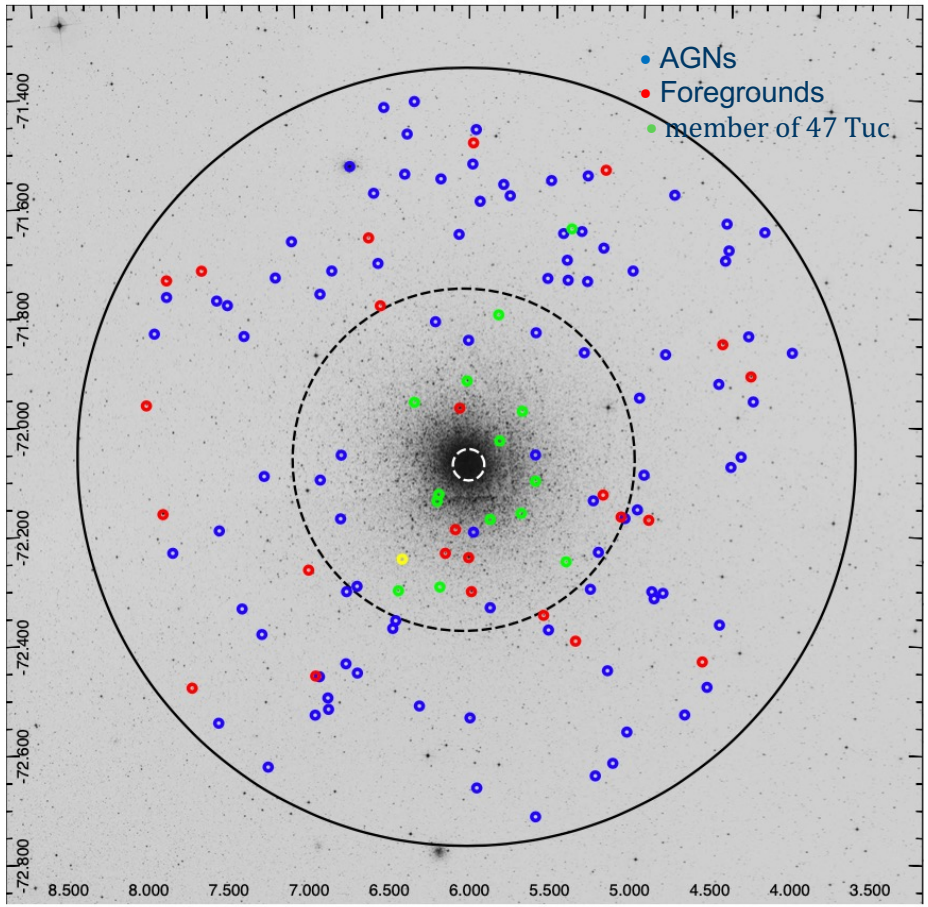


The optical image of the field of 47 Tuc observed by DSS survey. **We classified 2 symbiotic star, 2 QLMXBs, 3 CVs, 6 contact binaries, 96 AGNs, 25 foreground stars, 18 soft sources (<2.0keV) and 85 hard sources (>2.0keV).**

Saeedi et al, 2021, submitted in A&A

# Dwarf spheriodal galaxies (dSphs)

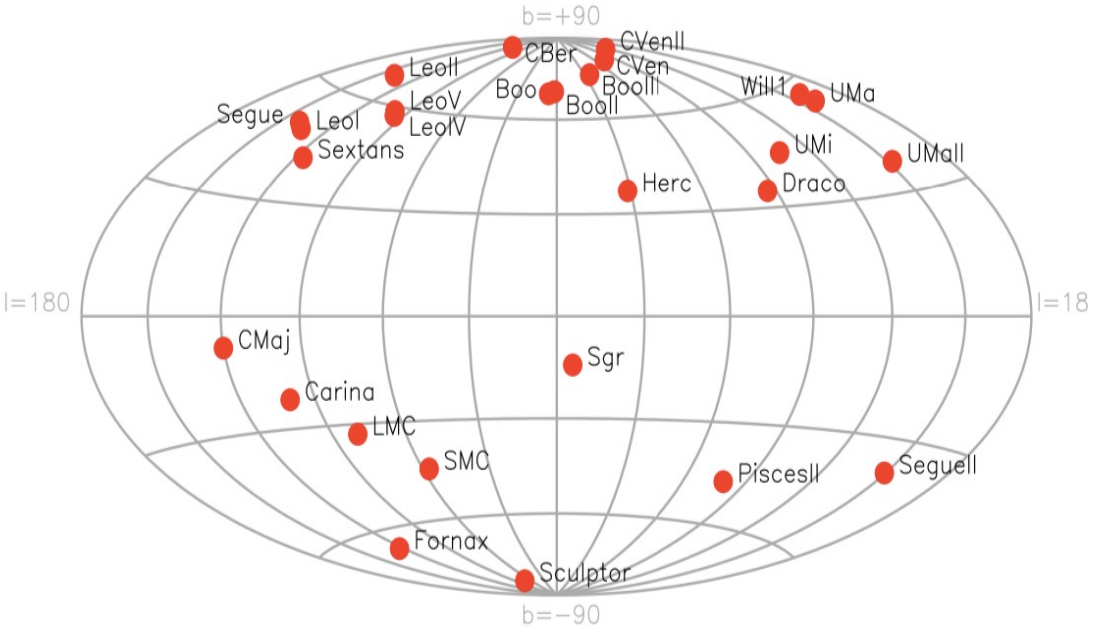


Aitoff projections of the Galactic coordinates of the Milky Way galactic satellites. (McConnachie , AJ, 2012)

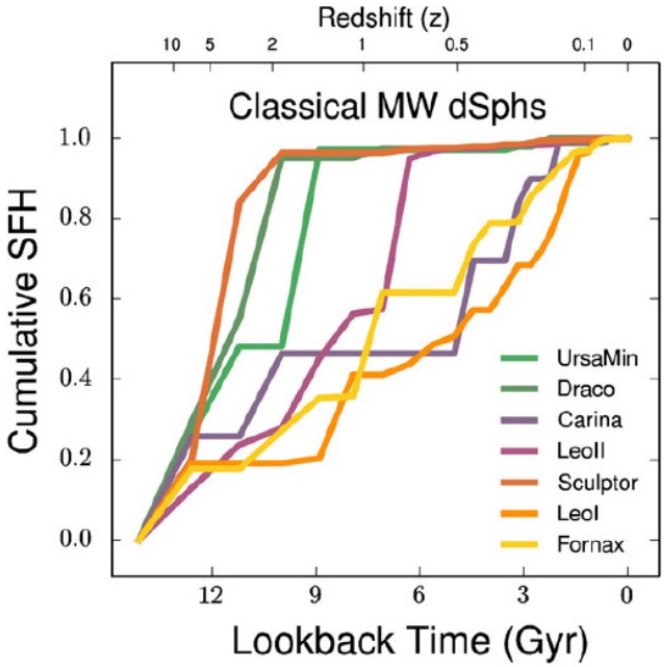


Cumulative star formation history of classical Milky Way dSphs (Weitz, et al. 2014).

# Updated list of properties of nearby dSphs

| Name | Distance Kpc | $r_h$ arcmin | M $10^6\ M_\odot$ |
|---|---|---|---|
| Canis major | 7±1 | 1200'. | 40. |
| Sagittarius | 26±2 | 342'.0 | 21. |
| Segue I | 23±2 | 4'.40 | 0.00034 |
| Ursa Major II | 32±4 | 16'.0 | 0.0041 |
| Reticulum II | 32±2 | 6'.0 | 0.056 |
| Triangulum II | 30±2 | 3'9 | 0.0007 |
| Segue II | 35±1 | 3'.40 | 0.00086 |
| Willman 1 | 38±1 | 2'.3 | 0.0010 |
| Bootes II | 42±1 | 4'.2 | 0.0010 |
| Coma Berenices | 44±4 | 6'.0 | 0.0037 |
| Bootes III | 47±2 | 2'.3 | 0.017 |
| Bootes I | 66±2 | 12'.0 | 0.029 |
| Draco | 76+6 | 10'.0 | 0.29 |

| Name | Distance Kpc | $r_h$ arcmin | M $10^6\ M_\odot$ |
|---|---|---|---|
| Ursa Minor | 76±3 | 8'.2 | 0.29 |
| Sculptor | 86±6 | 11'.3 | 2.3 |
| Sextans I | 86±4 | 27'.8 | 0.44 |
| Ursa major I | 97±4 | 11'.3 | 0.014 |
| Carina | 105±6 | 8'.20 | 0.38 |
| Hercules | 132±12 | 8'.6 | 0.037 |
| Fornax | 147±12 | 16.'6 | 20 |
| Leo IV | 154±12 | 4'.6 | 0.019 |
| Canes Venatici II | 160±4 | 1'.6 | 0.0079 |
| Leo V | 178±10 | 2'.6 | 0.011 |
| Pisces II | 182±15 | 1'10 | 0.0086 |
| Canes Venatici I | 218±10 | 8'.9 | 0.23 |
| Leo II | 233±14 | 2'.6 | 0.74 |
| Leo I | 254±15 | 3'.4 | 5.5 |

McConnachie, AJ,2017; Simon et al., APJ, 2015; Kirbyet al, APJ, 2015; Grillmair, APJ, 2009; Martin et al, MNRAS, 2004

# Low luminosity X-ray sources in dwarf galaxies

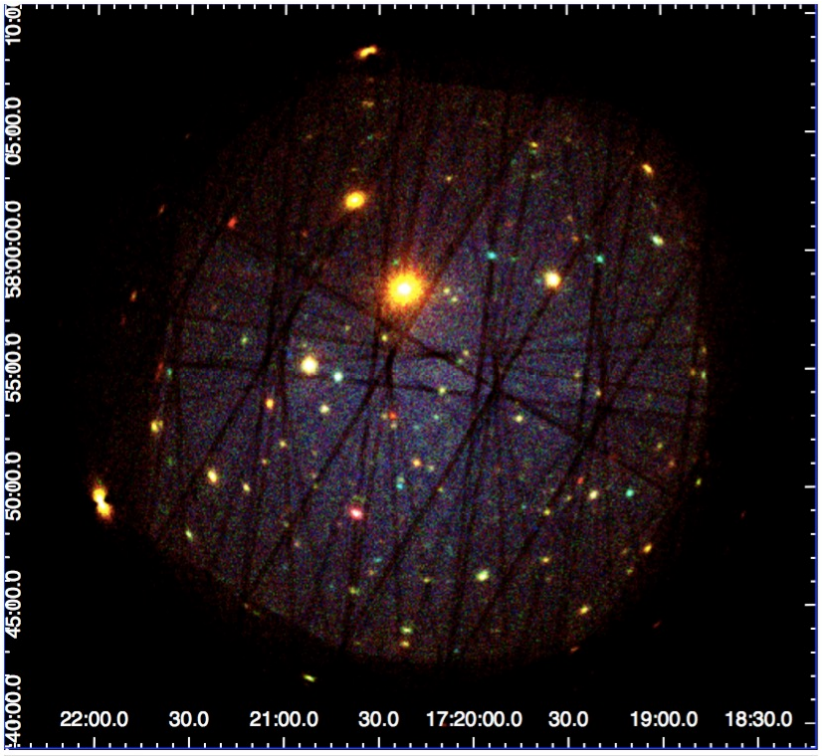


Draco dSph has been observed by *XMM-Newton* over 26 deep observations in 2015. (Saeedi et al. 2019, A&A)

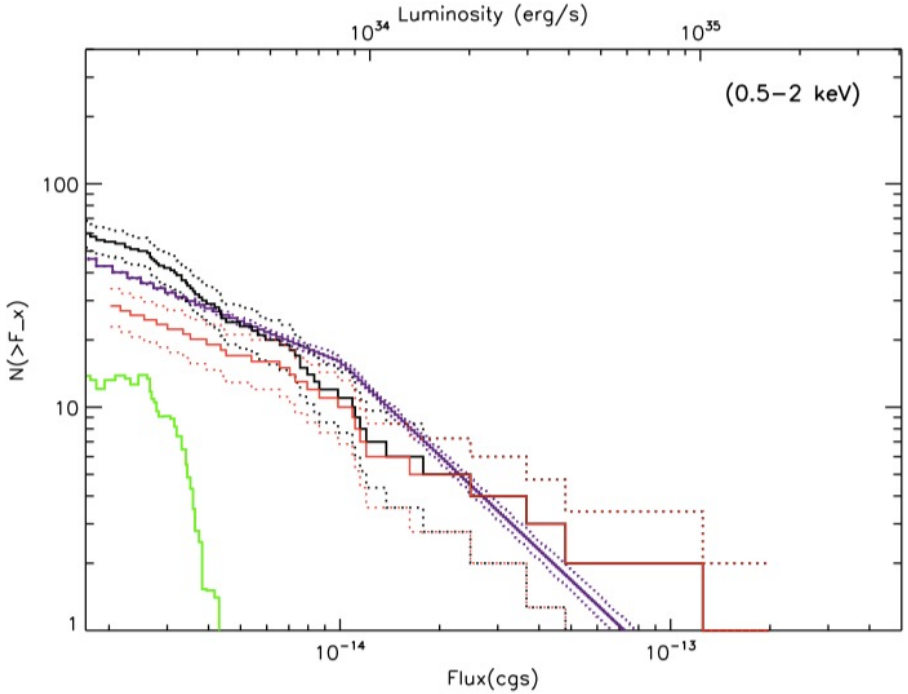


Cumulative X-ray luminosity function of the Draco dSph corrected for incompleteness in 0.5-2 keV.

**Back line:** Total detected sources corrected for incompleteness
**Purple line:** XMM-COSMOS function of AGNs scaled for the area of XMM EPICs of the Draco dSph.
**Green line:** **X-ray luminosity function (AGNs-subtracted).** (Saeedi et.al, 2016, A&A )

# Accreting White Dwarfs in the Draco dSph

- Draco dSph with a mass of **$0.29\times10^6\ M_\odot$** is located at **~76 kpc**.

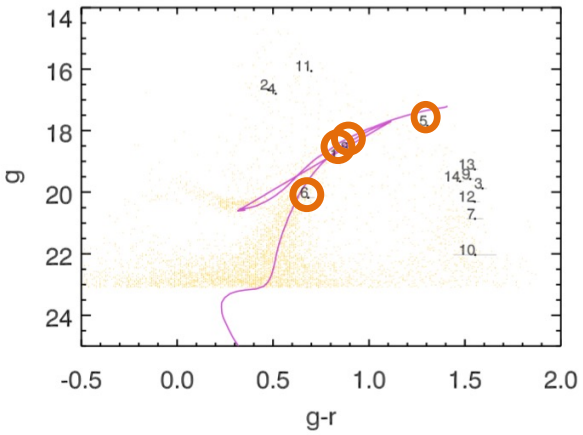


X-ray sources with stellar optical counterpart observed in 26 *XMM-Newton* observations of 2015.

**Yellow dots:** Members ($g$ < 23 mag) of the Draco dSph. (Rave et al. 2003).
**Violet line:** Stellar isochrone for age ($10^{10}$ yr) (Girardi et al. 2004)

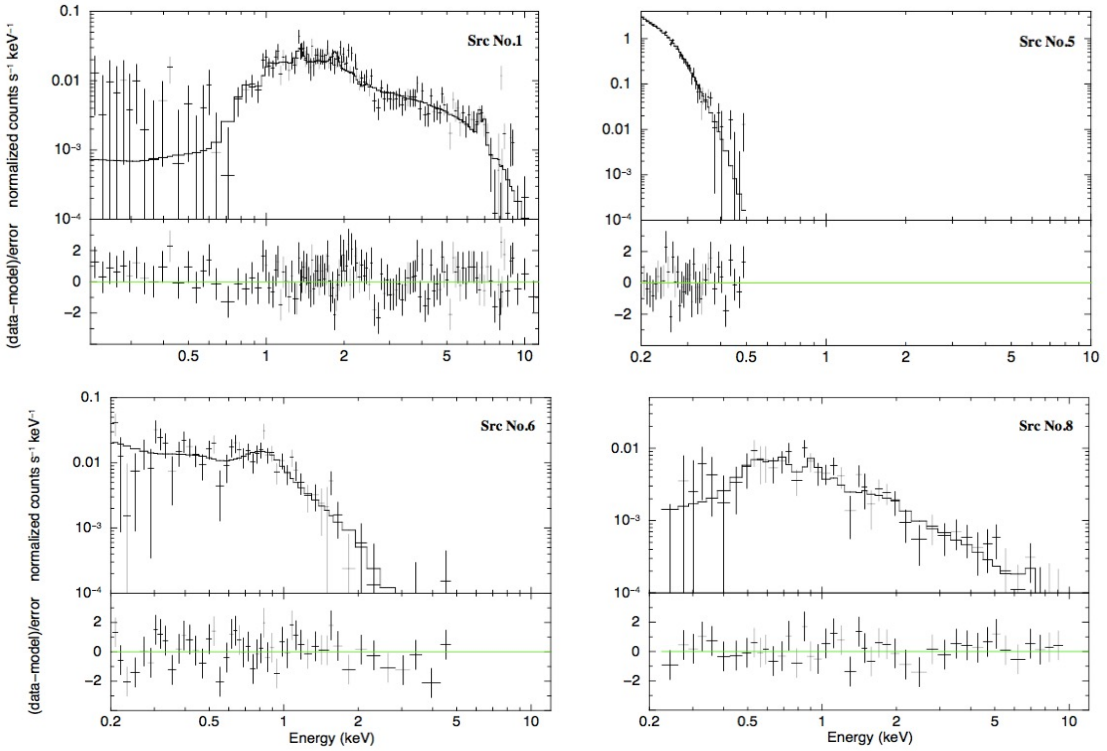


Spectra of the symbiotic stars in the Draco dSph. We have found one X-ray symbiotic binary candidate, one super soft source, and two $\beta$-type symbiotic stars.
(Saeedi et al. 2018, MNRAS, 2019, A&A).

# Accreting White Dwarfs in the Willman 1 dSph

- Willman dSph with a mass of **0.001×10⁶** $M_{\odot}$ is located at **~40 kpc**.

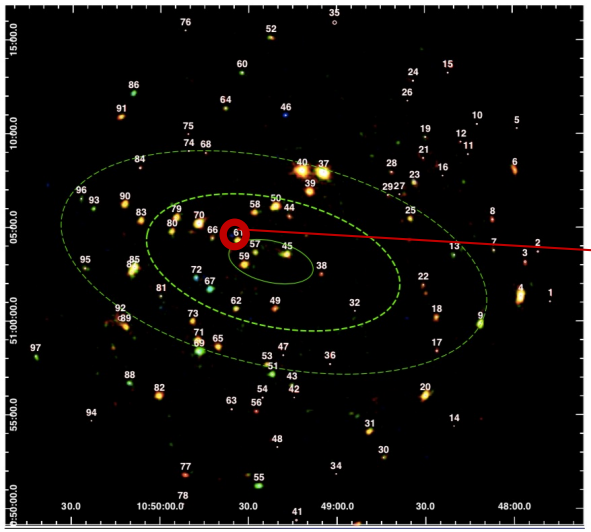

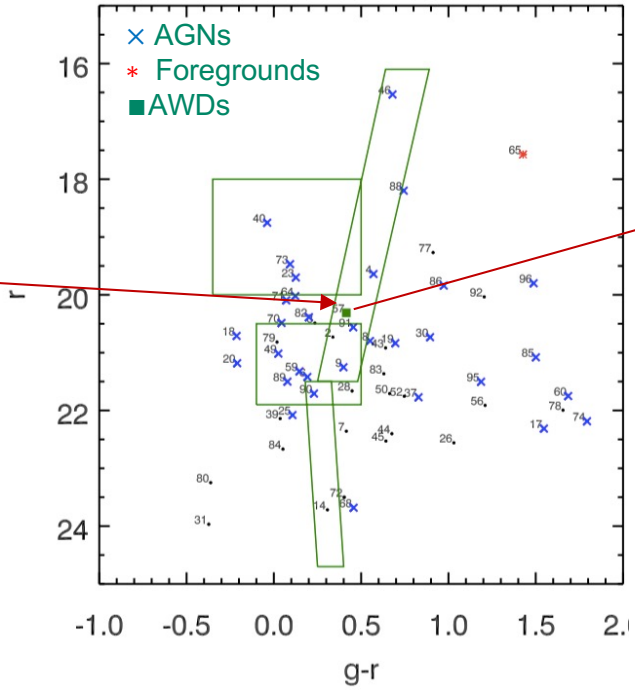


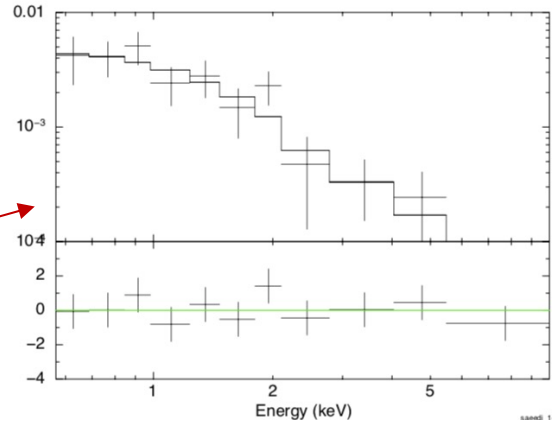


Colour-magnitude diagram (*g* versus *g* − *r* ) of the optical (SDSS9) counterparts of X-ray sources in the FOV of Willman 1 dSph. The region inside the green boxes is the isochrones of stellar population of Willman 1 dSph according to the criteria of Willman et al. (AJ, 2011, 142).

X-ray spectral analysis parameter Absorbed plasma model:
$N_H < 1.6\times10^{21}$
$KT$: $5.5^{+9.6}_{-3.4}$
abundance fixed to 0.1 solar abundance
Luminosity ~ $7.\times10^{32}$ erg/s
soft X-ray emission suggests that the source is a $\beta$-type symbiotic binary.

Saeedi et al., MNRAS, 2020.

# Low luminosity X-ray sources in the Sculptor dSph

FRIEDRICH-ALEXANDER UNIVERSITÄT ERLANGEN-NÜRNBERG
FACULTY OF SCIENCES

- Sculptor dSph with a mass of **$2.3\times10^6$** $M_\odot$ is located at **~86 kpc**.

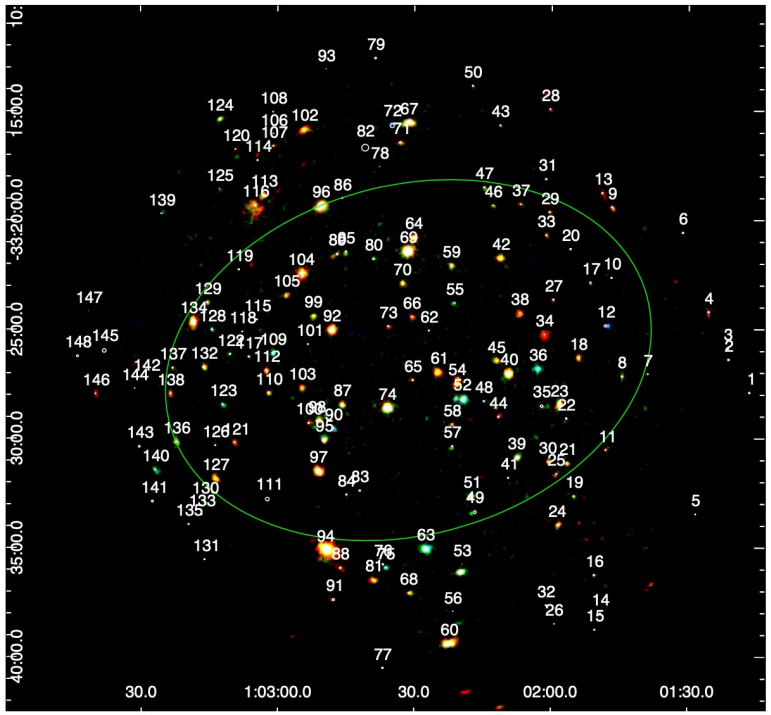


Three-colour mosaic image of Sculptor dSph. The green ellipse shows the main area of Sculptor dSph using the half-mass radius.

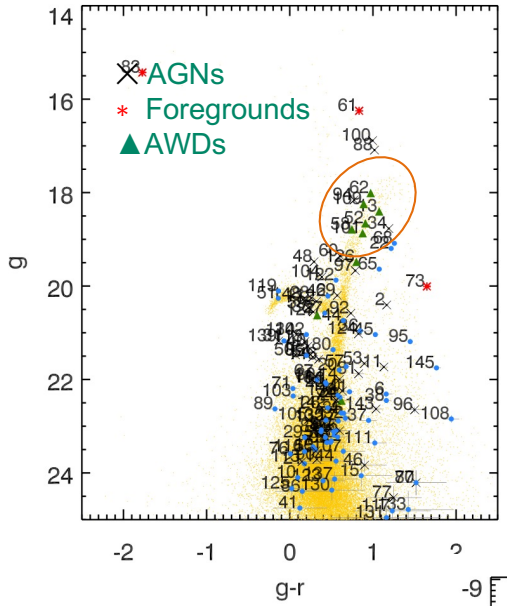


The optical counterpart of the X-ray sources in the field of Sculptor dSph. The yellow dots are all optical sources detected in the first data release of dark energy survey (Abbott et al. 2018) in the field of Sculptor dSph.

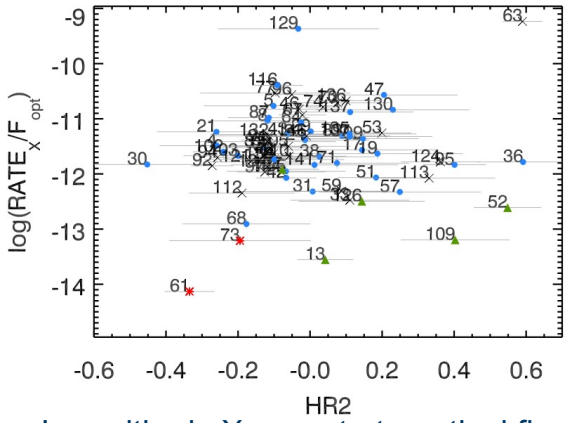


Logarithmic X-ray rate to optical flux ratio over the hardness ratio

- 6 symbiotic stars and 2 QLMXBs have been classified in the sculptor dSph.

Saeedi et al, 2021, submitted in MNRAS

# Low luminosity X-ray sources in Canis Major dwarf galaxy

FRIEDRICH-ALEXANDER UNIVERSITÄT ERLANGEN-NÜRNBERG
FACULTY OF SCIENCES

- Canis Major dSph with a mass of **40.×10⁶ $M_\odot$** is located at **~7 kpc**.

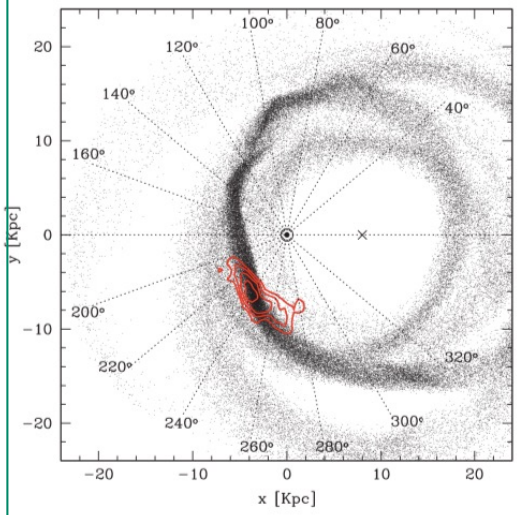


Red region show excess density contours of CMa (Bellazzini et al., MNRAS, 2006), which is plotted over the N-body simulation of the accretion of the CMa to the Milky Way viewed from the North Galactic Pole (Martin et al., MNRAS, 2005).

- *eROSITA* (eRASS1 and 2)detected ~18k sources in this region.
- ~800 sources are candidte as they have counterpart classfied as canis major dsph member

**(Theresa Heindl, Bachelor thesis)**

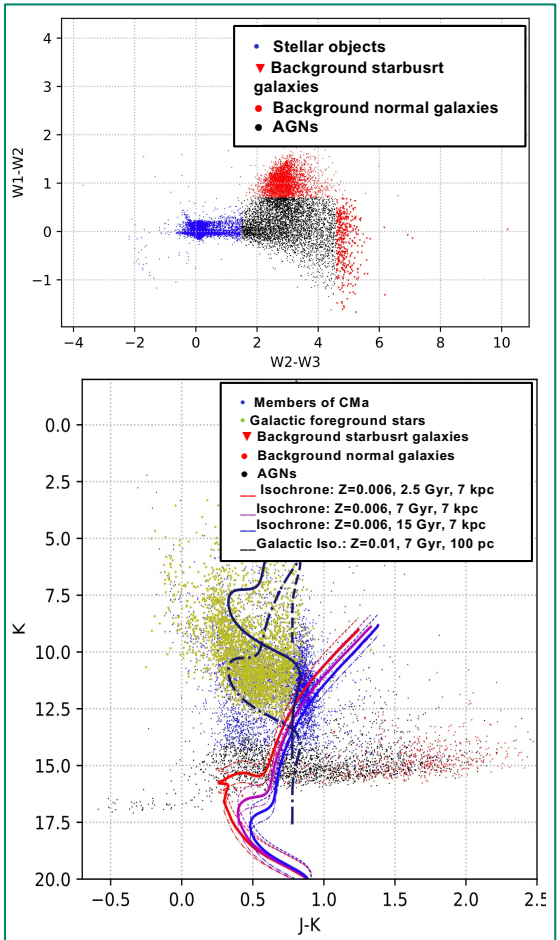


Upper plot: Colour-colour diagram of mid-infrared WISE counterparts.
Lower plot: colour magnitude diagram of 2MASS infrared counterparts.

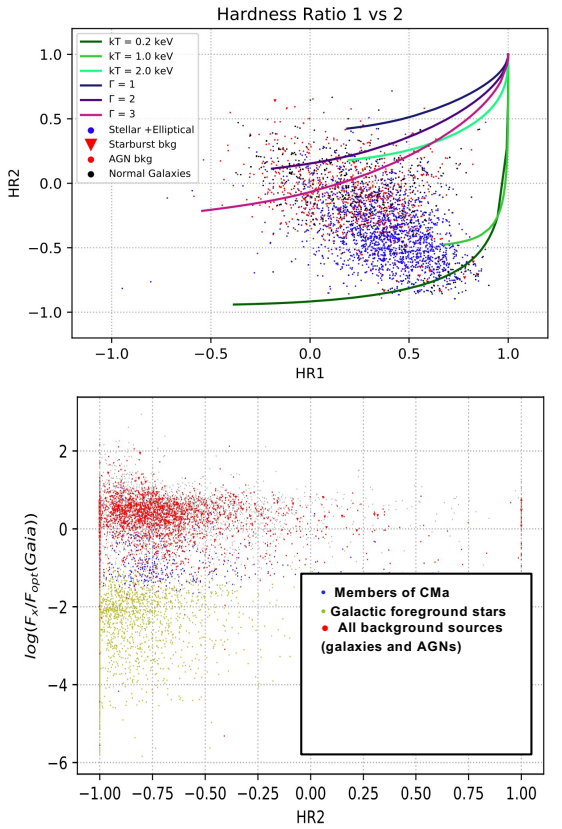


Upper plot: Hardness ratio of detected sources in the field of Canis Major dSph.
lower plot:Logarithmic X-ray rate to optical flux ratio over the hardness ratio

# *Summary and future works:*

- The old populations of dSphs and globular clusters are ideal labs for the study of low luminosity X-ray sources.
- The study of 47 Tuc globular cluster with *eROSITA* observations shows that there plenty of low luminosity X-ray sources belong to the globular cluster, however, out of its half mass radius. The main part of the sources have a luminosity $<10^{32}$ erg/s.
- The results of the classification of X-ray sources in different nearby dSphs show that the AWDs and QLMXBs are the main population of X-ray sources. No persistent LMXB has been found so far.
- *eROSITA* data of nearest dSphs e.g, Canis major and Sagittarius dSphs will help to perform a comparative study between the X-ray sources of globular clusters and dSphs.